

1 Charmless B Decay Measurements at Belle II

2 **Sagar Hazra**

3 *Tata Institute of Fundamental Research,*

4 *Mumbai 400 005, India*

5 *E-mail: sagar.hazra@tifr.res.in*

We report the measurements of CP asymmetry and branching fraction of various charmless B decays at the Belle II experiment. We use a sample of electron-positron collisions at the $\Upsilon(4S)$ resonance delivered by the SuperKEKB collider that corresponds to 62.8 fb^{-1} of integrated luminosity. All the results agree with the previous determinations and contribute important information to an early assessment of Belle II performance.

11th International Workshop on the CKM Unitarity Triangle (CKM2021)

November 22–26, 2021

The University of Melbourne, Australia

1. Introduction

The study of charmless B decays is a keystone of the flavor physics program to test the standard model (SM) and its extension. These decays mediated by Cabibbo-suppressed $b \rightarrow u$ tree and $b \rightarrow d, s$ loop transitions are sensitive to non-SM contributions. The CKM angle α/ϕ_2 can be measured directly only by an analysis of charmless $B \rightarrow \pi\pi, \rho\rho$ decays related by isospin symmetry. Isospin symmetry can be used also to make sum-rules, i.e. linear combination of \mathcal{B} and CP asymmetries of charmless decays, that can provide test of the standard model with precision generally better than 1%. Belle II has a unique capability of studying jointly, and within a consistent experimental environment for, all relevant final states of isospin-related B decays to improve the knowledge of α and put stringent bound on sum-rule tests.

Belle II [2] is a magnetic spectrometer having almost 4π solid-angle coverage, designed to reconstruct final-state particles of e^+e^- collisions delivered by the SuperKEKB asymmetric-energy collider [3], located at the KEK laboratory in Tsukuba, Japan. Belle II experiment started collecting data from March 2019. In this proceeding, we will focus on the result based on 62.8 fb^{-1} dataset which was collected at $\Upsilon(4S)$ resonance. With this dataset, charmless B decay mainly focus the early assessment of detector performance and advance analysis techniques capabilities.

2. Analysis overview and Challenges

We form final-state particle candidate by applying loose baseline selection criteria and then combine them in kinematic fits consistent with the topologies of the desired decays to reconstruct intermediate states and B candidates. The key challenge in reconstructing significant charmless signal is the large contamination from $e^+e^- \rightarrow q\bar{q}$ ($q = u, d, s, c$) continuum background coupled with low signal branching fraction. We use a binary-decision-tree classifier that combines a number of mostly topological variables having some discrimination between B -meson signal and continuum background. We pick up those variables whose correlation with E and M_{bc} is below $\pm 5\%$ to reduce possible bias in the signal yield determination. The latter two are the energy difference $E = E^* - \sqrt{s}/2$ between the energy of the reconstructed B candidate and half of the collision energy, both in the $\Upsilon(4S)$ frame, and the beam-energy-constrained mass $M_{bc} = \sqrt{s/(4c^4) - (p^*/c)^2}$, which is the invariant mass of the B candidate with its energy being replaced by the half of the center-of-mass collision energy. Another challenge is to separate B background events that peak in the signal region. To deal with this peaking background, we either kinematically veto it from the sample or include a separate component in the fit model. For example, in the analysis of $B \rightarrow K\pi\pi$ decays the background from $B^+ \rightarrow \bar{D}^0(\rightarrow K^+\pi^-)\pi^+$ decays is suppressed by vetoing candidates with a kaon-pion mass in the range $[1.84, 1.89] \text{ GeV}/c^2$. We then apply optimized continuum suppression and particle identification criteria. For the signal reconstruction efficiencies calculation and fit model development, we use simulation and correct/validate with control data. To determine the systematic uncertainties, pseudo-experiment and control channel studies are performed. We then inspect the most interesting region (or, signal region) on data to measure the physics observables.

3. Isospin sum-rule

The isospin sum-rule relation for the $B \rightarrow K\pi$ system given in Eq. (1) provides a stringent test of the SM.

$$I_c = \mathcal{A}_{c^-} + \mathcal{A}_{c^+} \frac{\mathcal{B}(K^0\pi^+) \tau_0}{\mathcal{B}(K^+\pi^-) \tau_+} - 2\mathcal{A}_{c^0} \frac{\mathcal{B}(K^+\pi^0) \tau_0}{\mathcal{B}(K^+\pi^-) \tau_+} - 2\mathcal{A}_{c^0} \frac{\mathcal{B}(K^0\pi^0)}{\mathcal{B}(K^+\pi^-)} = 0. \quad (1)$$

In all the four $K\pi$ channels, signal yields are determined with unbinned extended maximum-likelihood fits of the E and M_{bc} distributions. The key challenge in $B^0 \rightarrow K^0\pi^0$ analysis arises due to the absence of primary charged final-state particles at the B decay vertex. The position of the B vertex reconstructed from the intersection of the K_ℓ^0 trajectory with the interaction region. We measure the time-integrated asymmetry of the CP -eigenstate $B^0 \rightarrow K^0\pi^0$ with the signal-side quark flavor q obtained using the flavor content of the other B -meson, provided by the category-based flavor tagger [4]. The asymmetry \mathcal{A}_{c^0} is determined from a simultaneous maximum-likelihood fit to the unbinned $M_{bc} - E - q \cdot r$ distributions, where r is the dilution factor of flavor tagger output. The signal probability density function (PDF) is given by

$$\mathcal{P}_{\text{sig}} = \frac{1}{2} [1 + q(1 - 2w_A) \cdot (1 - 2\chi_3)\mathcal{A}_{c^0}], \quad (2)$$

where χ_3 is the $B^0 - \bar{B}^0$ mixing frequency, w_A is the wrong tag fraction in each dilution (r) interval. Figures 1 and 2 show the E distribution of all the four $K\pi$ system. We obtain the following branching fractions,

$$\begin{aligned} \mathcal{B}(B^0 \rightarrow K^+\pi^-) &= [18.0 \pm 0.9(\text{stat}) \pm 0.9(\text{syst})] \times 10^{-6}, \\ \mathcal{B}(B^+ \rightarrow K^+\pi^0) &= [11.9_{-1.0}^{+1.1}(\text{stat}) \pm 1.6(\text{syst})] \times 10^{-6}, \\ \mathcal{B}(B^+ \rightarrow K^0\pi^+) &= [21.4_{-2.2}^{+2.3}(\text{stat}) \pm 1.6(\text{syst})] \times 10^{-6}, \\ \mathcal{B}(B^0 \rightarrow K^0\pi^0) &= [8.5_{-1.6}^{+1.7}(\text{stat}) \pm 1.2(\text{syst})] \times 10^{-6} \end{aligned}$$

and CP -violating rate asymmetries

$$\begin{aligned} \mathcal{A}_{\%}(B^0 \rightarrow K^+\pi^-) &= -0.16 \pm 0.05(\text{stat}) \pm 0.01(\text{syst}), \\ \mathcal{A}_{\%}(B^+ \rightarrow K^+\pi^0) &= -0.09 \pm 0.09(\text{stat}) \pm 0.03(\text{syst}), \\ \mathcal{A}_{\%}(B^+ \rightarrow K^0\pi^+) &= -0.01 \pm 0.08(\text{stat}) \pm 0.05(\text{syst}), \\ \mathcal{A}_{\%}(B^0 \rightarrow K^0\pi^0) &= -0.40_{-0.44}^{+0.46}(\text{stat}) \pm 0.04(\text{syst}). \end{aligned}$$

The dominant contribution in the systematic uncertainties comes from π^0 and K_ℓ^0 reconstruction efficiency, it will be reduced with more data.

4. CP violation in multibody decays

The study of multibody [5] charmless B decays has recently attracted significant attention in the flavor program. The contribution between weak- and strong-interaction dynamics in $B^+ \rightarrow K^+K^-K^+$, $B^+ \rightarrow K^+\pi^-\pi^+$ and $B^0 \rightarrow K^+\pi^-\pi^0$ decays are enriched by the amplitude structure

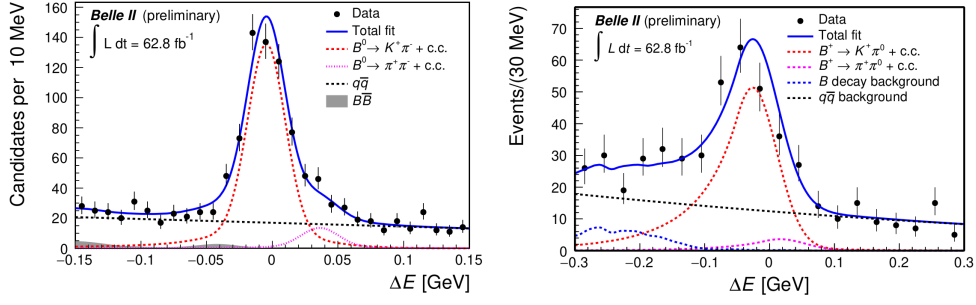


Figure 1: Signal-enhanced E distributions of $B^0 \rightarrow K^+ \pi^-$ (left) and $B^+ \rightarrow K^+ \pi^0$ (right).

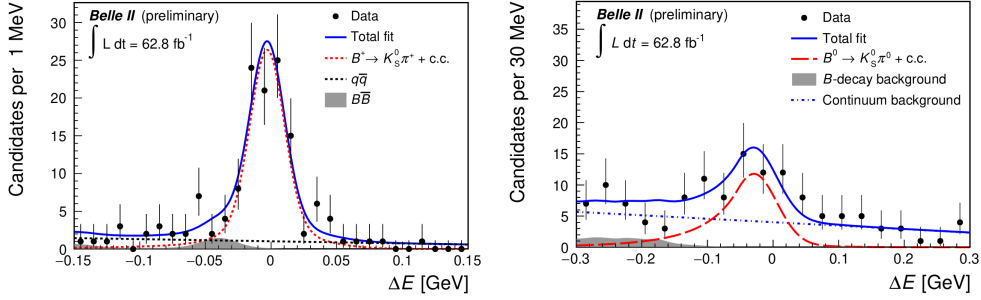


Figure 2: Signal-enhanced E distributions of $B^+ \rightarrow K^0 \pi^+$ (left) and $B^0 \rightarrow K^0 \pi^0$ (right).

66 accessible via their Dalitz plot. In Fig. 3 we show the E distributions for two of these multibody
 67 systems. We obtain the following branching fractions,

$$\begin{aligned} \mathcal{B}(B^+ \rightarrow K^+ K^- K^+) &= [35.8 \pm 1.6(\text{stat}) \pm 1.4(\text{syst})] \times 10^{-6}, \\ \mathcal{B}(B^+ \rightarrow K^+ \pi^- \pi^+) &= [67.0 \pm 3.3(\text{stat}) \pm 2.3(\text{syst})] \times 10^{-6}, \\ \mathcal{B}(B^0 \rightarrow K^+ \pi^- \pi^0) &= [38.1 \pm 3.5(\text{stat}) \pm 3.9(\text{syst})] \times 10^{-6} \end{aligned}$$

68 and CP -violating rate asymmetries

$$\begin{aligned} \mathcal{A}_{\%}(B^+ \rightarrow K^+ K^- K^+) &= -0.103 \pm 0.042(\text{stat}) \pm 0.020(\text{syst}), \\ \mathcal{A}_{\%}(B^+ \rightarrow K^+ \pi^- \pi^+) &= -0.010 \pm 0.050(\text{stat}) \pm 0.021(\text{syst}), \\ \mathcal{A}_{\%}(B^0 \rightarrow K^+ \pi^- \pi^0) &= +0.207 \pm 0.088(\text{stat}) \pm 0.011(\text{syst}). \end{aligned}$$

69 The dominant contribution in the systematic uncertainties comes from π^0 reconstruction and
 70 tracking efficiency, it will be reduced with more data.

71 5. Towards the determination of α/ϕ_2

72 The study of charmless decays at Belle II can provide improved measurements of the CKM
 73 unitarity angle $\alpha/\phi_2 = \arg -\frac{+c_{3+}^* +_{21}}{+D_{3+} +_{D1}^*}$, where $V_{\delta\gamma}$ are elements of the quark-mixing matrix. In
 74 particular, the combined analysis of branching fractions and CP violating asymmetries of the
 75 complete set of $B \rightarrow \pi\pi, \rho\rho$ isospin partners enables a determination of α [6]. We are now focusing

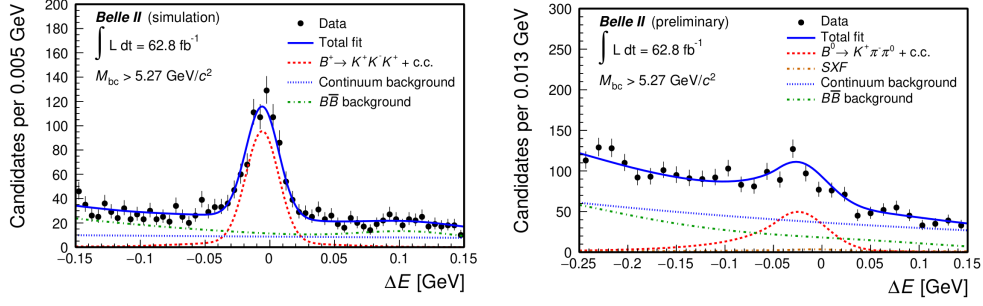


Figure 3: Signal-enhanced E distributions of $B^+ \rightarrow K^+K^-K^+$ (left) and $B^0 \rightarrow K^+\pi^-\pi^0$ (right).

76 on $B^0 \rightarrow \pi^0\pi^0$, $B^+ \rightarrow \pi^+\pi^0$, $B^0 \rightarrow \pi^+\pi^-$ and $B^+ \rightarrow \rho^+\pi^0$ decays. The $B^0 \rightarrow \pi^0\pi^0$ channel is
 77 particularly challenging as it requires two π^0 reconstruction. A dedicated boosted decision-trees
 78 classifier used to suppress background photons by combining 20 calorimetric variables. Signal
 79 yields are determined with an extended maximum-likelihood fit of the E , M_{bc} and transformed
 80 continuum suppression variable. Figure 4 shows the E distribution of two $\pi\pi$ channels. We obtain
 81 the following branching fractions,

$$\begin{aligned}\mathcal{B}(B^0 \rightarrow \pi^+\pi^-) &= [5.8 \pm 0.7(\text{stat}) \pm 0.7(\text{syst})] \times 10^{-6}, \\ \mathcal{B}(B^+ \rightarrow \pi^+\pi^0) &= [5.5^{+1.0}_{-0.9}(\text{stat}) \pm 0.7(\text{syst})] \times 10^{-6}, \\ \mathcal{B}(B^0 \rightarrow \pi^0\pi^0) &= [0.98^{+0.48}_{-0.39}(\text{stat}) \pm 0.27(\text{syst})] \times 10^{-6}\end{aligned}$$

82 and CP asymmetry of $\mathcal{A}_{\%}(B^+ \rightarrow \pi^+\pi^0) = -0.04 \pm 0.17(\text{stat}) \pm 0.06(\text{syst})$. The $B^+ \rightarrow \rho^+\rho^0$
 83 decay involves pion-only final state, where the large width of the ρ mesons offers reduced distinctive
 84 features against dominant continuum background. Isolating a low-background signal is therefore the
 85 main challenge of the analysis. Signal yields are determined with an unbinned maximum-likelihood
 86 fits of E , continuum-suppression decision-tree output, the dipion masses and cosines of helicity
 87 angles of the ρ candidates. Figure 5 shows the E and log transform continuum-suppression output
 88 of $B^+ \rightarrow \rho^+\rho^0$ candidates. We obtain the branching fraction $\mathcal{B} = [20.6 \pm 3.2(\text{stat}) \pm 4.0(\text{syst})] \times 10^{-6}$
 and longitudinal polarization fraction $f_l = 0.936^{+0.049}_{-0.041}(\text{stat}) \pm 0.021(\text{syst})$. The dominant

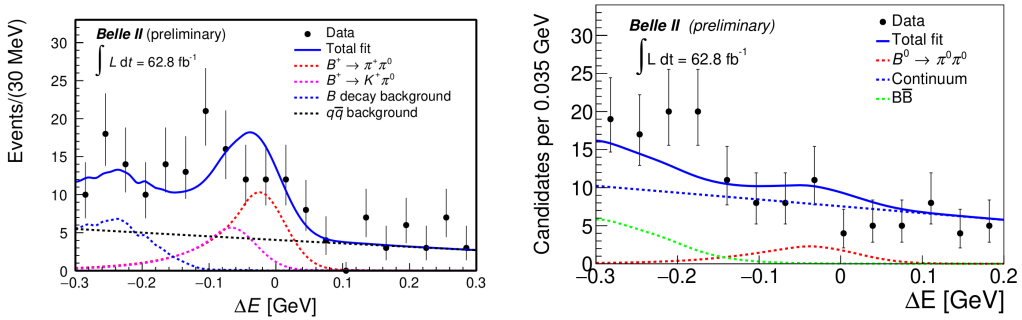


Figure 4: Signal-enhanced E distributions of $B^+ \rightarrow \pi^+\pi^0$ (left) and $B^0 \rightarrow \pi^0\pi^0$ (right).

89 contribution in the systematic uncertainties comes from π^0 reconstruction and tracking efficiency,
 90 it will be reduced with more data.
 91

